九州工業大学学術機関リポジトリ
Kyutacar
Kyushu Institute of Technology Academic Repository

# Altitude dependent failure rate calculation for high power semiconductor devices in aviation electronics



| 著者 | Gollapudi Srikanth, Omura Ichiro |
|---|---|
| journal or publication title | Japanese Journal of Applied Physics |
| volume | 60 |
| number | SB |
| page range | SBBD19-1-SBBD19-7 |
| year | 2021-04-13 |
| URL | http://hdl.handle.net/10228/00008803 |

doi: https://doi.org/10.35848/1347-4065/abebc0

# Altitude dependent failure rate calculation for high power semiconductor devices in aviation electronics

Srikanth Gollapudi[1]*, Ichiro Omura[1]

[1]*Kyushu Institute of Technology, 2-4, Hibikino, Wakamatsu-ku, kitakyushu 808-0196, Japan*

E-mail: gollapudi.srikanth108@mail.kyutech.jp

The electric power usage in aircraft has reached 1MW. Therefore, use of high power semiconductor devices expected to increase in avionics. Single Event Burnout (SEB) failure happens when power devices operating in blocking condition interact with the cosmic radiation. The failure rate in power devices is more in airplane altitude compare to terrestrial operation. In this paper, the failure rate of high power silicon PiN diode operating in airplane altitude due to the interaction of cosmic ray neutrons. The proposed formula has the unique feature of decoupling between failure cross section and cosmic ray neutron flux. This makes it possible to calculate the failure rate under any cosmic radiation environment using the proposed failure rate formulation.

## 1. Introduction

The need for minimizing operating and maintenance costs of aircraft have encouraged the aircraft industry to move towards electric aircraft. As a result, the usage of electric power on-board of aircraft has reached 1 MW. [1] This ever increase in usage of electric power in aircraft causes major changes in electric power system architecture and increases the demand for high power semiconductor devices.[2] The high power semiconductor devices (e.g. BJTs, MOSFETs, and diodes etc.) used in space, avionics, and terrestrial systems interacts with energetic particles. These energetic particles deposit its energy in the device by creating electron-hole pairs over a distance of some micrometers. During the conduction state of a device, the deposited extra charge carriers do not affect the device. However, in the blocking state, the plasma of induced charge carriers shields its interior from the electric field. The voltage drop occurs at pronounced field spikes at the edge of plasma. When these field spikes exceed the critical electric field of the device material, leads to the further generation of carriers due to impact ionization. This phenomenon induce a destructive mechanism in power devices called single event burnout (SEB).

Early observation of SEB in power devices was in power MOSFETs when exposed to heavy ion. [3] Power MOSFET burnout has attributed to the parasitic bipolar transistor inherent to the MOSFET structure. Numerous studies have revealed the susceptibility to single event burnout resulting in catastrophic failure in MOSFET when operating in cosmic ray environment. [4-7] Later, burnout failures in bipolar transistors was reported [8].

Subsequently, power diode and GTO vulnerability to SEB was reported [9-11], a localized breakdown observed in the bulk of a device.[12-13] However, the mechanism for SEB failure in power diode was different from BJT. It was reported that avalanche multiplication caused the SEB failure in power diodes without bipolar transistor action and occurs at a voltage much below the avalanche breakdown voltage. [14-17]

The intensity of neutron flux changes with the altitude and reaching a maximum between 15 km to 20 km, called Pfotzer maximum. [18-20] Also observed that, neutron intensity is 80-150 times higher at Pfotzer maximum than at sea level.[21] The plot of measured in-flight upset rates against altitude and latitude correlated with the atmospheric neutron variation as function of altitude and latitude. [22] Therefore, the atmospheric neutron are the dominant radiation environment for catastrophic failure in aviation electronics. [23]

The knowledge of failure rate in high power semiconductor devices plays a crucial role before choosing the rating of components in aviation electronics. Failure rates usually

measured in FIT. One FIT corresponds to a failure in one billion hours of device operation. A phenomenological expression for calculation of failure rate in silicon devices was proposed [24] due to the impact of terrestrial neutrons. The modification to this method applicable for SiC power devices proposed from neutron irradiation experimental data. [25] Many irradiation experiments conducted to observe the device failure[26-28] and the failure rate calculated for an inverter shown at different application conditions including elevated altitude.[29] The failure rate calculation method for SiC power MOSFET by considering the threshold energy deposition as failure criteria of MOSFET. [30]

In this paper, a decoupled failure rate calculation method is proposed for high power semiconductor devices applicable to any cosmic ray operating conditions such as terrestrial, airplane altitude and satellite orbit. [31-34] PiN diode is considered because of presence of PiN structure in all high voltage semiconductor devices. Threshold charge considered as failure criteria for device destruction. In this paper, the altitude dependent failure rate in 100μm and 300μm PiN diode is shown due to the impact of neutron up to an altitude of 60 km. The failure cross section data for the 100μm and 300μm calculated using the proposed method is considered from sudo et al.[33] in the present work. The neutron flux spectrum required for SEB failure rate calculation considered from EXPACS database.

The neutron flux spectrum also varies with solar activity. Therefore, n the results for voltage corresponding to 1 FIT are shown over the duration of 25 years for 100μm and 300μm PiN diode at 10 km altitude due to neutron interaction. The effect of maximum cutoff energy of neutron spectrum on failure rate calculation also shown.

## 2. Proposed failure rate calculation methodology

Failure rate calculation involves dealing with solid-state physics, nuclear physics and radiation physics as shown in Fig. 1.

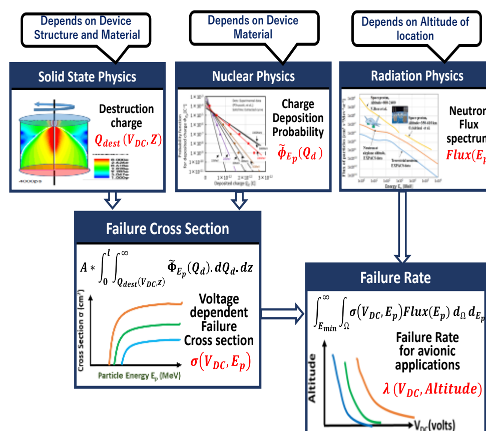


Fig. 1. Failure rate calculation

Threshold charge for device destruction considered as failure criteria of the device in the calculation of failure cross section. Failure cross section obtained by integrating threshold charge for device destruction and the probability of charge deposition in silicon by the cosmic ray particle. The calculated failure cross section is unique for the device. The failure cross section as a function of voltage and particle energy given in Eq. (1),

$$\sigma(V_{DC}, E_p) = A \int_0^l \int_{Q_{dest}(V_{DC},Z)}^{\infty} \tilde{\phi}_{E_p}(Q_d \ )dQ_d \, dz \qquad (1)$$

Where $\sigma$ = Failure cross section in $cm^2$

$V_{DC}$ = Applied voltage in Volts

$E_p$ = Energy of particle in MeV

A = Device area in $cm^2$

l = i-layer thickness in μm

$Q_{dest}$ = Critical amount of deposited charge in C

$\tilde{\phi}_{E_p}$ = Deposited charge probability in silicon in $C^{-1}cm^{-1}$

z = Position along depth direction in μm

The proposed failure rate calculation methodology formulated by introducing decoupling between failure cross section and the cosmic ray flux spectrum. So once the failure cross section known from Eq. (1), it is possible to obtain the failure rate (λ) of the device operating at any radiation condition. Failure rate calculation shown in Eq. (2).

$$\lambda = \int_{E_{min}}^{\infty} \int_{\Omega} \sigma(V_{DC}, E_p) Flux(E_p) \ \ d_{\Omega} \ \ d_{E_p} \qquad (2)$$

Where $\lambda$ = Failure rate in FIT

$\Omega$ = solid angle in sr

Flux = particle flux in $MeV^{-1}s^{-1}cm^{-2}\ sr^{-1}$

$E_{min}$ = minimum energy of particles in MeV

The failure rate in high power devices due to space protons[31)] calculated using the

proposed method. The failure rate in high power semiconductor device due to terrestrial neutrons[33] is shown by conducting heavy ion simulation at different locations along the PiN diode using the proposed methodology by considering the neutron spectrum from gordon et al [35]. The calculated failure rate compared with phenomenological expression proposed by Zeller[24] is shown in Fig. 2. It shows, the failure rate at high voltage region is good agreement with the experimental data of Zeller. In the present work, we focused on failure rate calculation in high voltage devices in avionics.

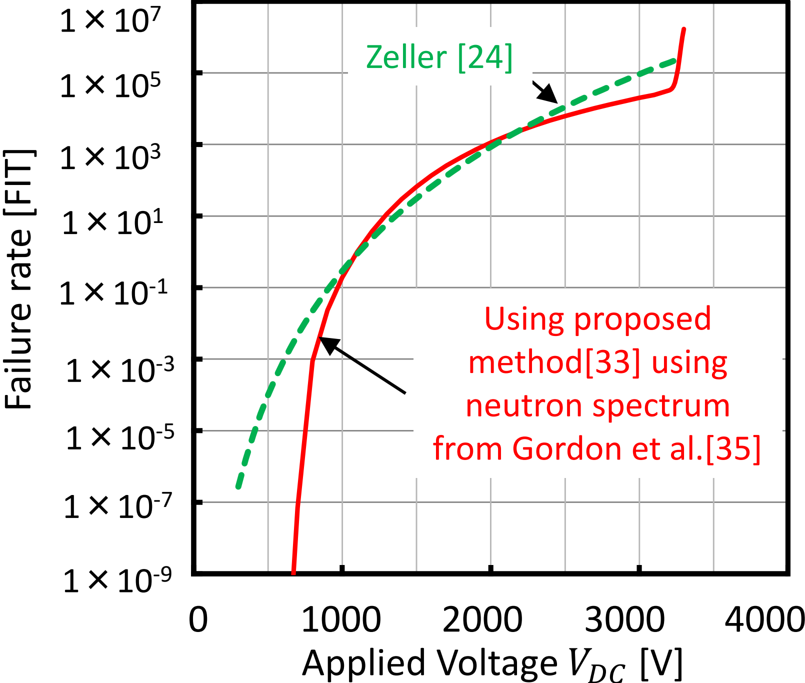


Fig. 2. Failure rate due to terrestrial neutrons

## 2.1 Neutron Flux spectrum at airplane altitude

The neutron flux spectrum up to 60 km altitude obtained from EXPACS data[36-39]. In this, the cosmic ray neutron spectrum calculated by performing a Monte Carlo particle transport simulation in the atmosphere. It based on the Particle and Heavy Ion Transport code System (PHITS). The neutron flux spectrum shown in Fig. 3.

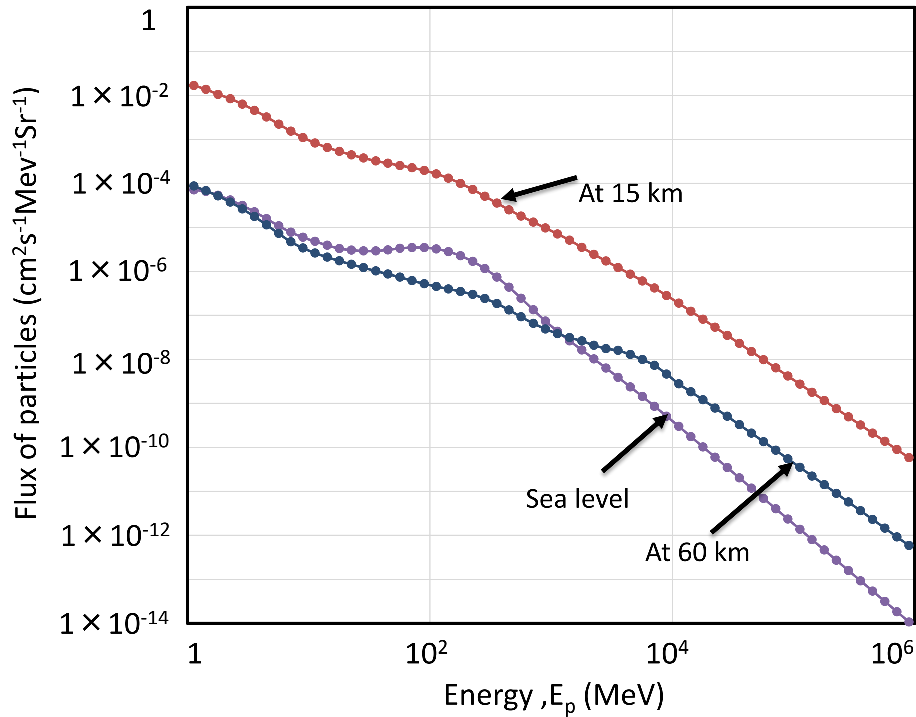


Fig. 3. Neutron flux spectrum up to 60 km altitude

It can observe from the figure that the neutron flux increases with altitude up to Pfotzer maximum. Commercial aeroplanes generally travel at altitude of around 10 km and rocket-powered aircraft such as X-15 can travel at higher altitudes. So power devices in avionics tend to interact more with cosmic ray neutron. In this paper, the failure rate is calculated for power devices operating up to an altitude of 60 km due to the interaction of cosmic ray neutrons over wide energy range shown in fig. 3.

## 2.2 Charge deposition probability

Probability of energy deposition in silicon by different energetic particles considered from literature.[40-42] Ionization energy required to generate the charge in silicon is 22.5 MeV/pC. [43] Using this relation, the energy deposition probability converted in to charge deposition probability in silicon. The extracted probability of charge deposition curves for different energies in silicon shown in Fig. 4 is considered from Sudo et al.[33] These extracted curves are compared with the experimental data from P Truscott et at.[40] represent as dots in the figure.

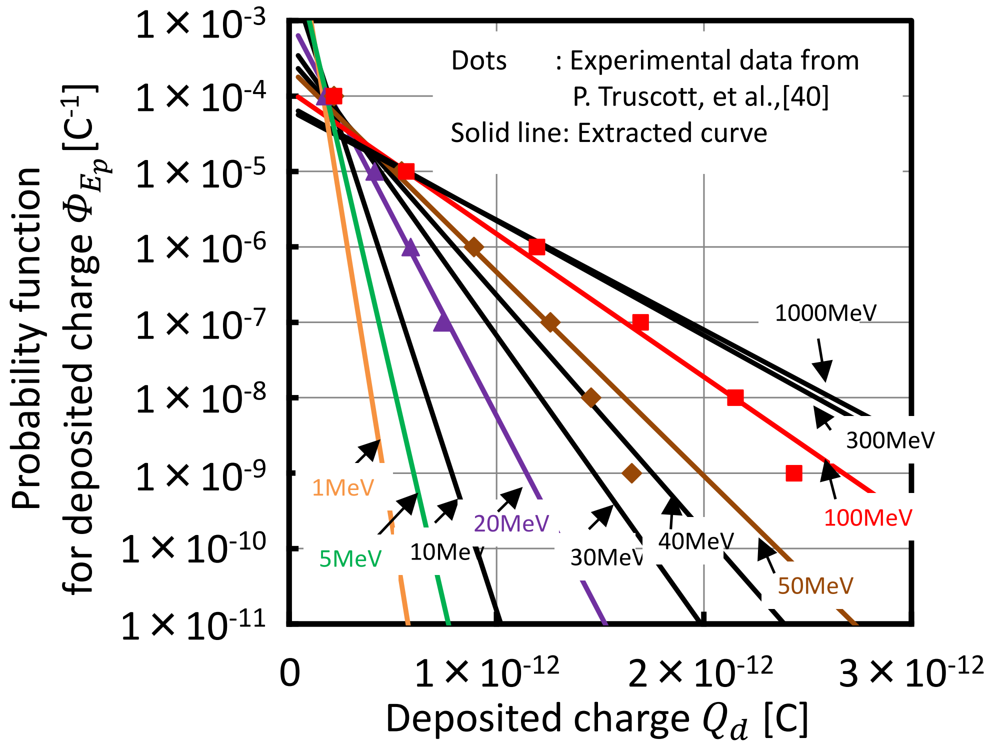


Fig. 4. Charge deposition probability in silicon [33]

### 2.3 Critical charge for device destruction

Destruction charge taken as criteria for device failure in the proposed method. Destruction charge ($Q_{dest}$) is nothing but the threshold of the generated charge that cause the device failure. In the failure rate calculation in SiC devices proposed by Ball et al[30] assumed the sensitive volume of the power device and the secondary particles. The proposed method based on the assumption of size of the initial deposited charge. In the cosmic ray induced failures in SiC device proposed by Akturk et al[25] , the failure cross section is obtained by performing terrestrial neutron experiments at Los Alamos Neutron Science Center (LANSCE) with particles up to 800 MeV energy. Whereas, failure cross section in the proposed method obtained from critical charge for device destruction and the energy deposition probability as shown in Eq. (1) over wide range of neutron energy as shown in Fig. 3. The generated charge obtained from TCAD simulation for different initial charge depositions. The initial charge deposition carried out at different locations along the PiN diode to obtain the critical charge for device destruction as a function of impact location. This is implemented by using heavy ion model for initial charge deposition and Van Overstraeten and de Man Model for Impact ionization in Sentaurus Devices simulator by synopsis. The generated charge obtained by initial deposited charge at PN junction in 300µm diode shown in Fig. 5. Similarly, the generated charge in 100µm diode for deposited charge

at PN junction shown in Fig. 6.

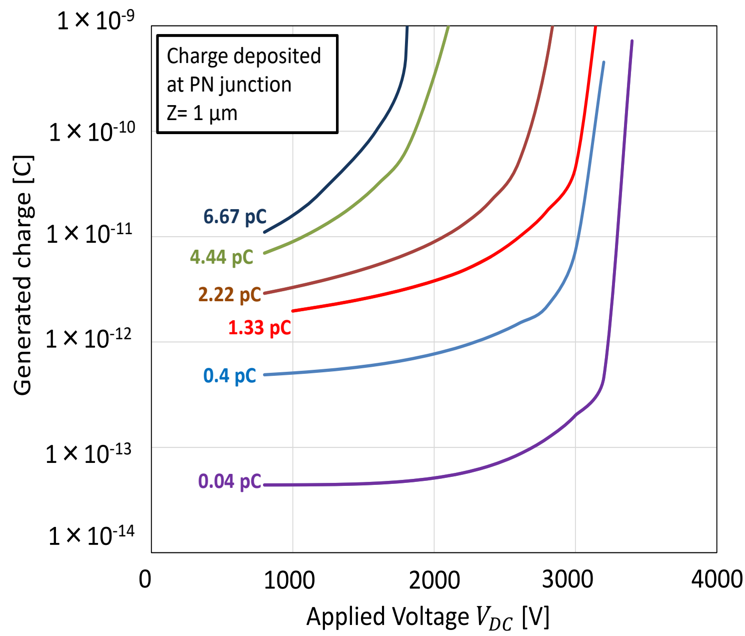


Fig. 5. Generated charge in 300µm diode when charge deposited at PN junction

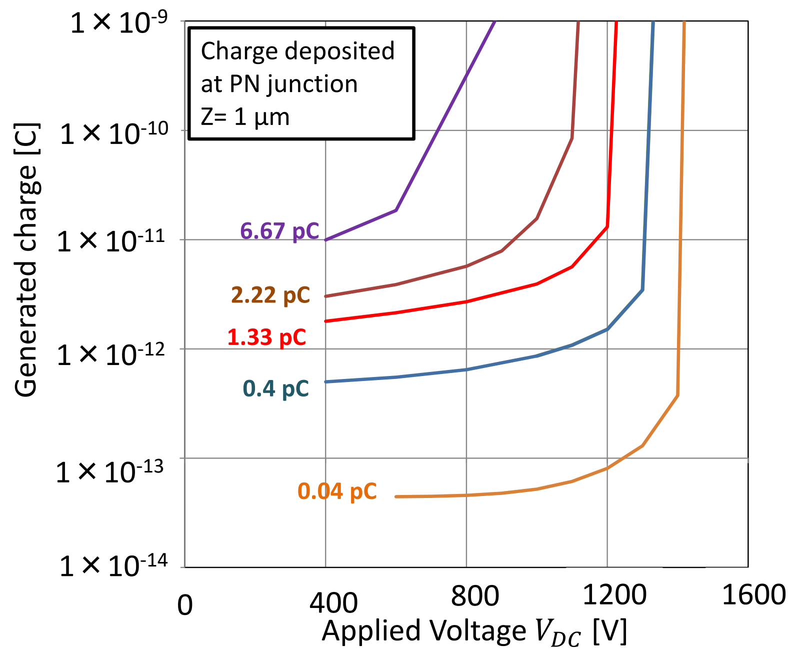


Fig. 6. Generated charge in 100µm diode when charge deposited at PN junction

The threshold charge for device destruction obtained from the generated charge profiles in Fig. 5 and Fig. 6. The threshold charge for device destruction at different locations along the PiN diode is shown in Fig. 7 and Fig. 8 are considered from sudo et al.[33)] The threshold charge for the device destruction increases as the deposited charge is away from the PN junction because of decrease the electric field. The obtained critical charge for device

destruction in 300µm PiN diode shown in Fig. 7.

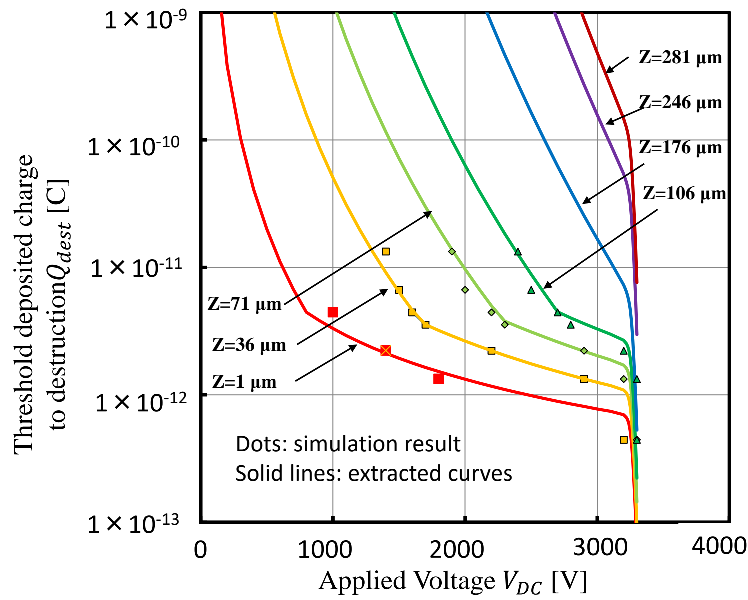


Fig. 7. Critical amount of charge for destruction in 300µm PiN diode

Similarly, the threshold charge for the device destruction evaluated from Fig. 6 for 100µm PiN diode shown in Fig. 8 for different initial charge deposition positions.

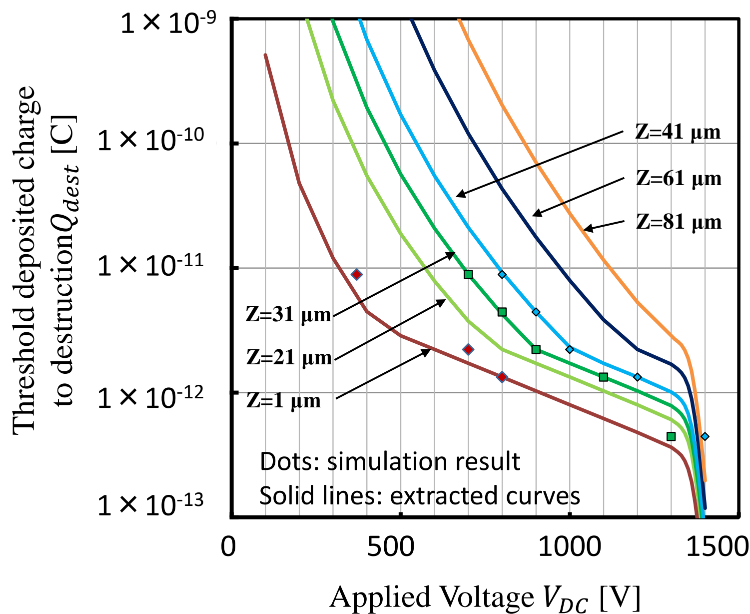


Fig. 8. Critical amount of charge for destruction in 100µm PiN diode

## 3. Failure cross section and failure rate calculation

Failure cross section evaluation using critical charge for device destruction and charge deposition probability shown in Eq. (1). The calculated failure cross section is unique for 300µm silicon PiN diode. Device cross section for different operating voltages of 300µm and 100 µm PiN diode obtained from sudo et al.[33] is shown in Fig. 9 and Fig.10 respectively.

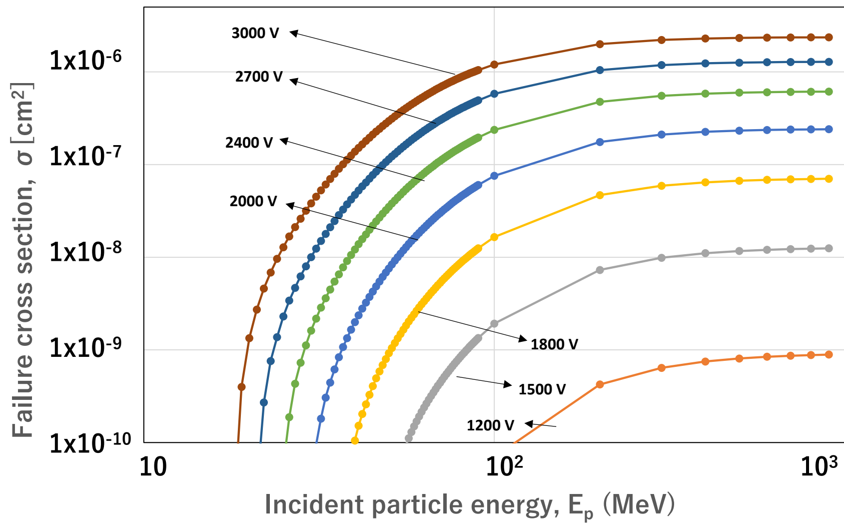


Fig. 9. Cross section σ [cm$^2$] of a 300μm PiN diode

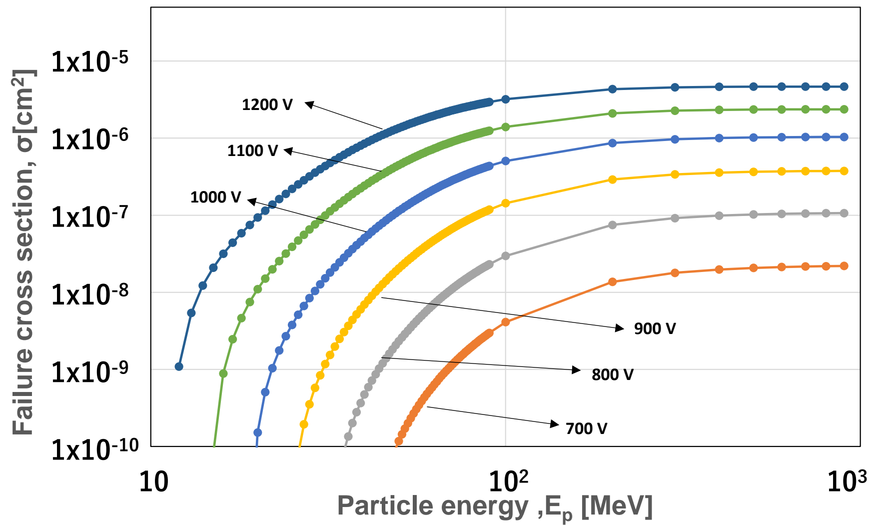


Fig. 10. Cross section σ [cm$^2$] of a 100μm PiN diode

Once the failure cross section of a device known, it is possible to calculate the failure rate of the device operating at any radiation condition using Eq. (2). The present work shows the calculated the failure rate due to cosmic ray neutrons when the device operating up to an altitude of 60 km.

The altitude dependent failure rate for 300μm PiN diode shown in Fig. 11. From this, it is clear that, the operating voltage corresponding to device destruction reduces at commercial airplane altitude compared to terrestrial operation.

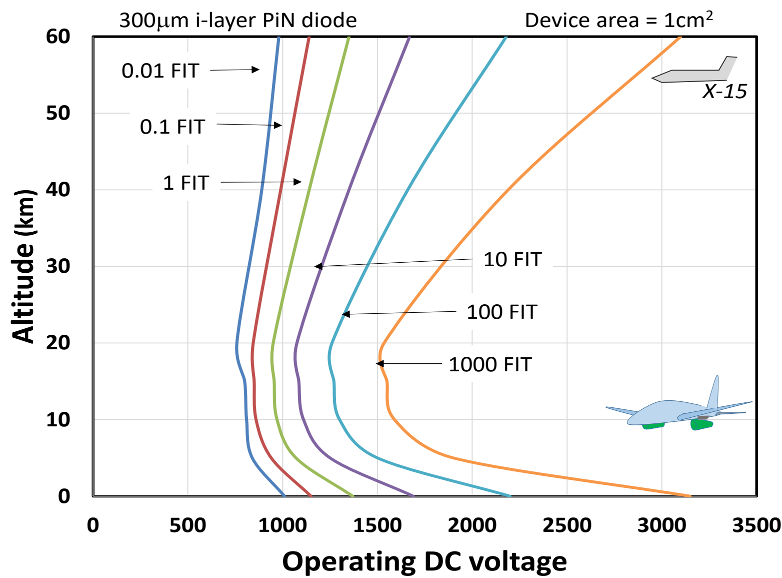


Fig. 11. Failure rate variation with altitude and operating voltage in 300μm PiN diode

Similarly, the altitude dependent failure rate calculated for 100μm PiN diode shown in Fig. 12.

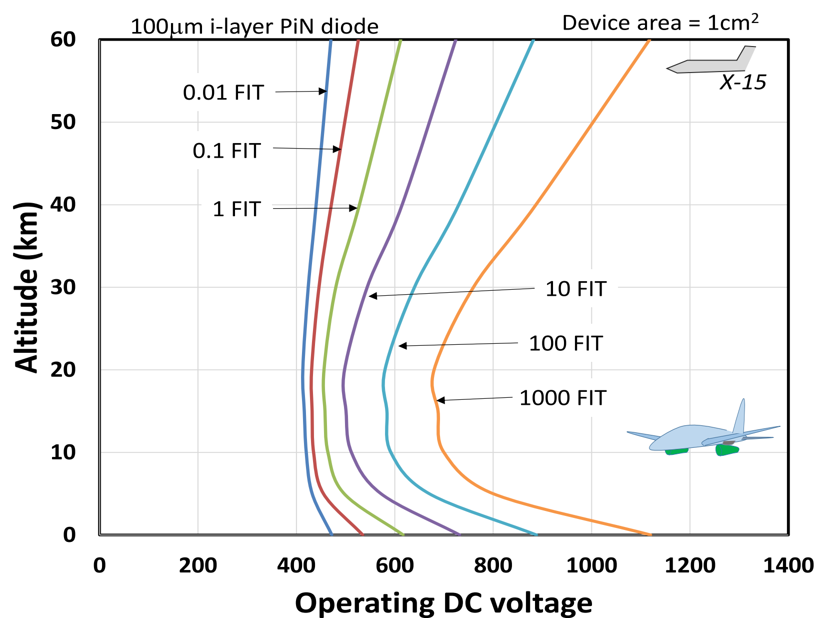


Fig. 12. Failure rate variation with altitude and operating voltage in 100μm PiN diode

From these results, it is clear that operating condition of the device plays a crucial role in selecting the rating of the power semiconductor. Therefore, proper selection of power device for avionics is very important in order to confine the failure rate in permissible limits.

The eleven-year solar cycle creates an additional magnetic field around the earth. This increases the shielding against intra-galactic cosmic rays and the atmospheric cosmic rays during the period of active sun. [19] So the neutron intensity decreases during active sun

and increases during quiet sun. The effect of this solar cycle on failure rate of device calculated for a period of 25 years from 1990 to 2015.

The range of voltage corresponding to a failure of 1FIT in 300μm diode shown in Fig.13 during different years of operation. Here the device operation considered at an altitude of 10 km when the cosmic ray neutrons interact with the device.

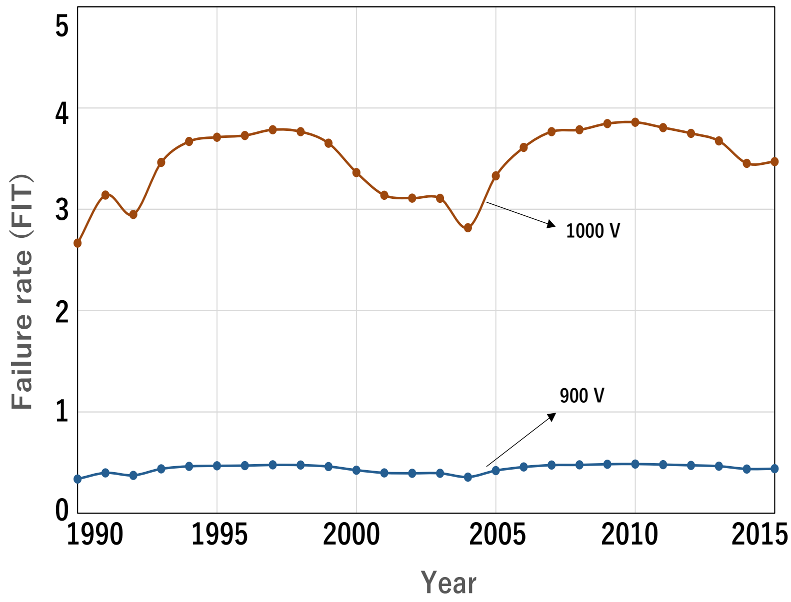


Fig. 13. Range of operating voltage for 1FIT in 300μm diode operating at 10 km altitude

Similarly, the range of operating voltage for a failure rate near to 1FIT in 100μm PiN diode during different years of operation is shown in Fig. 14.

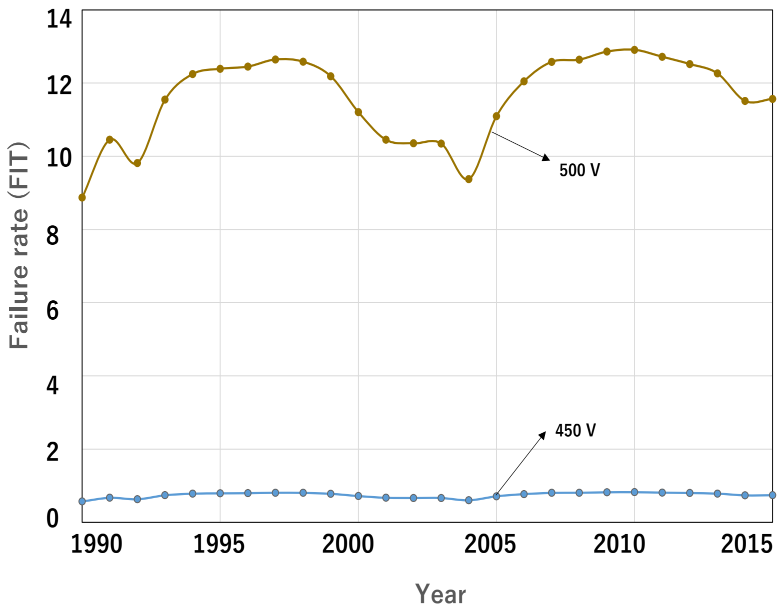


Fig. 14. Range of operating voltage for 1FIT in 100μm diode operating at 10 km altitude

Accelerating tests are conducted to evaluate the SEB failure rate of power devices. The accelerating test facilities have the limitation of maximum energy of the particles, eg. LANSCE facility has a maximum particle energy of 800 MeV, Tri-University Meson Facility (TRIUMF) has maximum energy of 520 MeV, Osaka research center for nuclear physics has facility of 400 MeV. The effect of low energy particles is critical to the failure when the power device operating near to breakdown voltage of device. However, when considering the de rating of power device in avionics, high energy particles shown significant effect on failure rate. To clarify this, the effect maximum cutoff particle energy on failure rate of the power device is evaluated.

The calculated failure rate at 10 km altitude at different maximum cutoff energy is shown in Fig. 15 for 300 µm PiN diode.

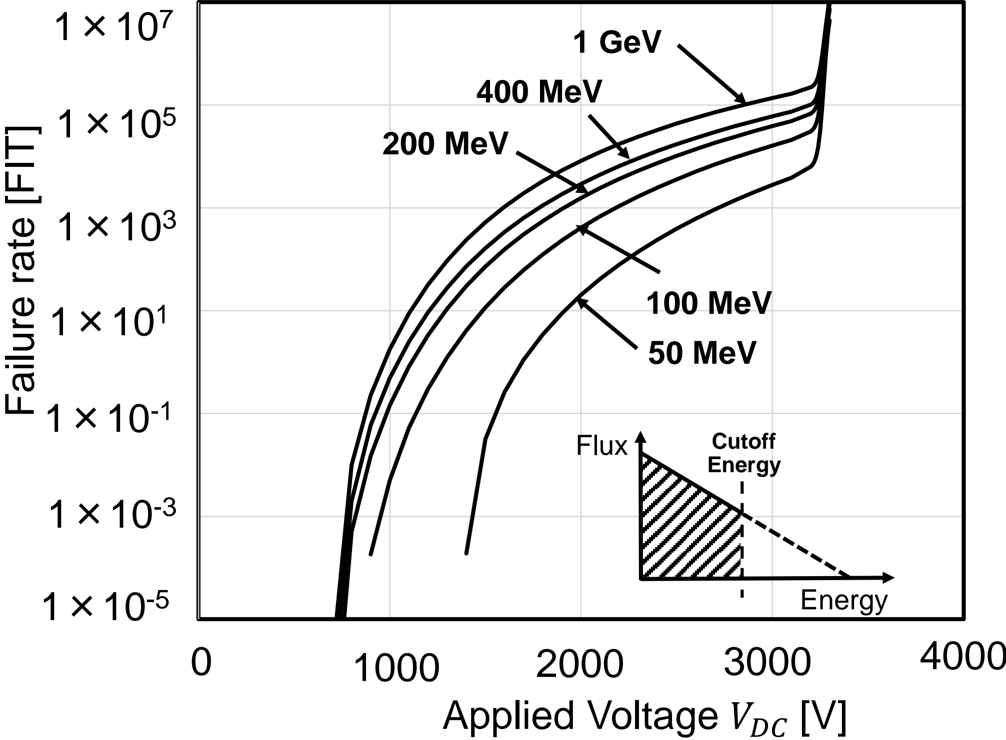


Fig. 15. Failure rate for different maximum energy cutoff in 300 µm PiN diode at 10 Km altitude

Similarly, the calculated failure rates in 100 µm PiN diode at different maximum cutoff energy is shown in Fig. 16.

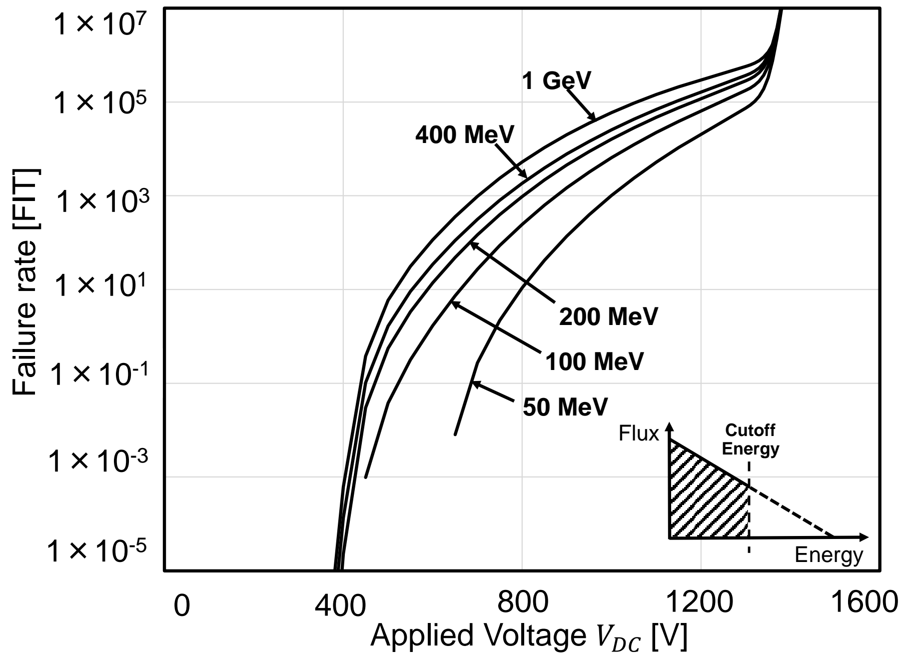


Fig. 16. Failure rate for different maximum energy cutoff in 100 µm PiN diode at 10 km altitude

From this, it is clear that, the high energy particles have significant effect on failure rate when the device operating at lower voltage levels compared to breakdown voltage region. This low voltage region is particularly important for avionic electronics. Under estimation of failure rate is observed with the omission of high energy particles in the failure rate calculation.

The factor of under estimation in failure rate for different maximum cutoff energy of the spectrum obtained as function of voltage. The under estimation factor is below one order of magnitude up to 400 MeV cutoff energy in the low voltage region of the device. However, this factor increases to two orders of magnitude for the cut off energy below 200 MeV at low voltage region of the power device. Since the power devices in avionic electronics operates in de rating condition, this low voltage region of the power device is particularly important. Therefore, the maximum cutoff energy of the spectrum plays an important role in calculating the failure rate of the power devices operating at avionic altitude. The under estimation factor in 300µm PiN diode for different maximum cutoff energy of the spectrum is shown in fig. 17.

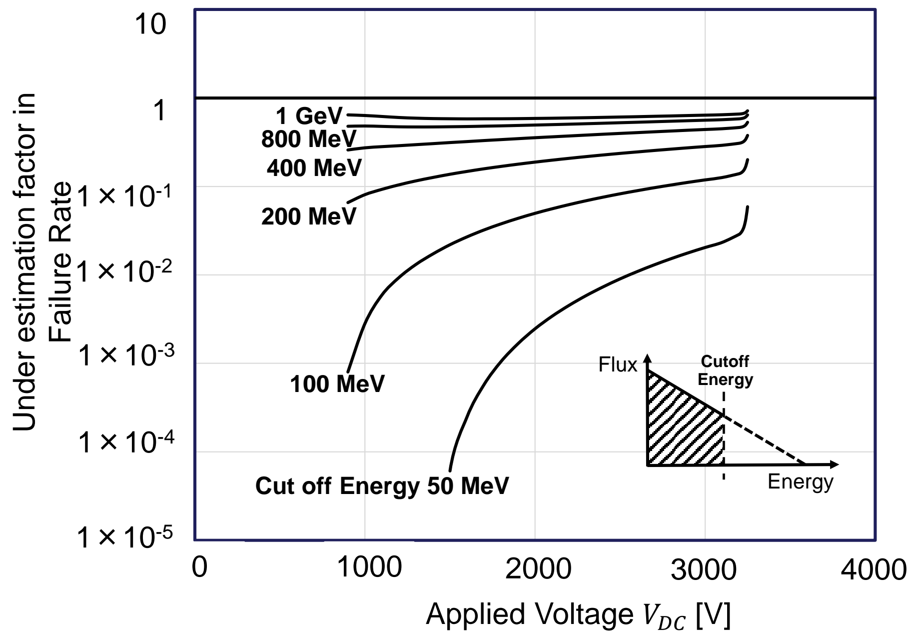


Fig.17. Under estimation factor of failure rate for different maximum cutoff energy of spectrum in 300 µm PiN diode at 10 Km altitude (Reference failure rate is due to complete spectrum shown in Fig.3)

Similarly, the failure rate under estimation factor for different maximum cutoff energy of spectrum is shown for 100 µm power diode in fig. 18.

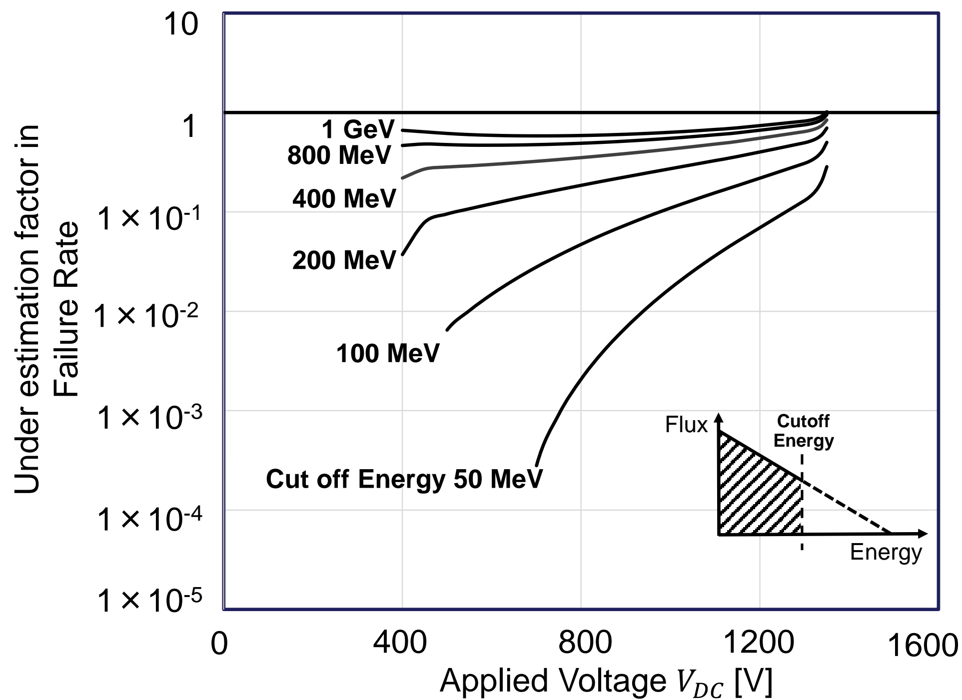


Fig.18. Under estimation factor of failure rate for different maximum cutoff energy of spectrum in 100 µm PiN diode at 10 Km altitude (Reference failure rate is due to complete spectrum shown in Fig.3)

## 4. Conclusions

This paper presents the methodology to calculate the failure rate of high power semiconductor device. The introduction of decoupling between failure cross-section and the neutron flux spectrum makes it possible to calculate failure rate for any radiation condition. Failure rate variation with altitude in 100μm and 300μm PiN diode is successfully demonstrated using neutron flux spectrum from EXPACS database up to 60 km altitude. Also evaluated the effect of solar cycle on the device failure rate. In addition, the effect of maximum cutoff energy on failure rate also demonstrated due to neutrons at 10 km altitude.

## References


1. V. Madonna, P. Giangrande, and M. Galea, IEEE Trans. Transportation Electrification 4, 646 (2018).
2. I. Moir and A. G. Seabridge, *Military Avionics Systems* (Wiley, New York 2006) p.399.
3. A.E.Waskiewicz, J.W.Groninger, V.H.Strahan, D.M.Long, IEEE Trans. Electron Devices 33, 1710(1986).
4. G. H. Johnson, J. H. Hohl, R. D. Schrimpf, and K. F. Galloway, IEEE Trans. Electron Devices 40, 1001(1993).
5. J. L. Titus, and C. F. Wheatley, IEEE Trans. Nucl. Sci. 43, 533(1996).
6. S. Kuboyama, S. Matsuda, T. Kanno, and T. Ishii, IEEE Trans. Nucl. Sci. 39,1698(1992).
7. S. Kuboyama, S. Matsuda, T. Kanno and T. Hirose, IEEE Trans. Nucl. Sci. 41, 2210(1994).
8. J. L. Titus, G. H. Johnson, R. D. Schrimpf, and K. F. Galloway, IEEE Trans. Nucl. Sci. 38,1315(1991).
9. H. Kabza, H.J. Schulze, Y. Gerstenmaier, P. Voss, J. Wilhelmi, W. Schmid, F.Pfirsch, and K.Platzoder, Proc. Int. Symp. Power Semiconductor Devices and ICs, 1994, p. 9.
10. H.Matsuda, T.Fujiwara, M.Hiyoshi, and K.Nishitani, Proc. Int. Symp. Power Semiconductor Devices and ICs, 1994, p. 221.
11. H.R.Zeller, Proc. Int. Symp. Power Semiconductor Devices and ICs, 1994, p. 339.
12. H.R.Zeller, Solid-State Electronic 38, 2041(1995).

13. A. M. Albadri, R. D. Schrimpf, D. G. Walker and S. V. Mahajan, IEEE Trans. Nucl. Sci. 52, 2194 (2005).
14. D.G. Walker, A.M. Albadri, T.S.Fisher, and R.D.Schrimpf, Proceedings of IMECE, 2002, p.17.
15. U. Scheuermann and U. Schilling, IET Power Electron. 9, 2027(2016).
16. K.H. Maier, A. Denker, P. Voss, H.W. Becker, Nucl. Instrum. Meth. B 146 ,596 (1998).
17. G.Soelkner, P. Voss, W. Kaindl, G. Wachutka, K.H. Maier, H.W. Becker, IEEE Trans. Nucl. Sci. 47, 2365(2000).
18. E. Normand, IEEE Trans. Nucl. Sci. 43, 461(1996).
19. J. F. Ziegler, IBM Journal of Research and Development 40, 19(1996).
20. M. Kole, M. Pearce, and M. Muñoz Salinas, Astropart. Phys. 62 ,230(2015).
21. P. Goldhagen, MRS Bulletin 28, 131 (2003).
22. J.L.Lerey, Microelectron. Reliab. 47, 1827(2007).
23. E. Normand and T. J. Baker, IEEE Trans. Nucl. Sci. 49, 1484(1993)
24. H. Zeller , Microelectron. Reliab. 37 , 1711(1997).
25. A. Akturk, M.McGarrity, N.Goldsman, D.J. Lichenwalner, B. Hull, D. Grider, and R. Wilkins, IEEE Trans. Nucl. Sci. 66, 1828(2019).
26. G.H. Johnson, J.M. Palau, C. Dachs, K.F. Galloway, R.D. Schrimph, IEEE Trans. Nucl. Sci. 43, 546(1996).
27. T. Shoji, S. Nishida, K. Hamada, and H. Tadano, IET Power Electronics 8, 2315(2015).
28. T. Shoji , S. Nishida, T. Ohnishi, T. Fujikawa, N. Nose, M. Ishiko, and K. Hamada, Int. Power Electronics Conf., 2010, p.142.
29. U. Schilling, Semikron Appl. Note AN 17-003, 2017.
30. D. R. Ball et al., IEEE Trans. Nucl. Sci. 66, 337(2019).
31. Erdenebaatar Dashdondog, Shohei Harada, Yuji Shiba and Ichiro Omura, Microelectronics Reliability 64, 494 (2016).
32. Y. Shiba, E. Dashdondog, M. Sudo, and I. Omura, Proc. Int. Symp. Power Semiconductor Devices and ICs, 2017, p.167.
33. M.Sudo, T. Nagamatsu, M. Tsukuda and I. Omura, Microelectronics Reliability 100–101 (2019).
34. Srikanth Gollapudi, Ichiro Omura, Solid State Devices and Materials, 2020, p.275.
35. M.S.Gordon, P.Goldhagen, K.P.Rodbell, T.H.Zabel, H.H.K. Tang, J.M.Clem,

P.Bailey, IEEE Trans. Nucl. Sci.51 , 3427(2004).
36. Tatsuhiko Sato and Koji Niita, Radiation Research 166, 544(2006).
37. T. Sato, Public Library Of Science ONE 11, e0160390 (2016).
38. T. Sato, Public Library Of Science ONE 10, e0144679 (2015).
39. EXPACS: EXcel-based Program for calculating Atmospheric Cosmic-ray Spectrum [http://phits.jaea.go.jp/expacs] / (2016).
40. P. Truscott, C. Dyer, A. Frydland, A. Hands, S. Clucas and K. Hunter, Proc. of RADECS, 2005, p. LN11.
41. B.Doucin, Y.Patin, J.P.Lochard, J.Beaucour, T.carriere, D.Isabelle, Buisson, T.Corbiere, and T.Bion, IEEE Trans. Nucl. Sci. 41, 593(1994).
42. B. Doucin, T. Carriere, C. Poivey, P. Garnier, J. Beaucour and Y. Patin, Proc. of RADECS, 1995, p. 402.
43. G.C. Messenger, Ash Milton, Single Event Phenomena (Springer, New York, 1997) p.133,164